Ecotoxicology and Environmental Safety 270 (2024) 115778

Contents lists available at ScienceDirect

Ecotoxicology and Environmental Safety

journal homepage: www.elsevier.com/locate/ecoenv

Mechanism through which the hsa-circ_0000992– hsa- miR- 936–AKT3 regulatory network promotes the $PM_{2.5}$-induced inflammatory response in human bronchial epithelial cells

Jing Lin Li [b,1], Yi Tan [a,1], Qiu Ling Wang [c,1], Cai Xia Li [a], Jin Chang Hong [a], Hong Jie Wang [a], Yi Wu [a], De Chun Ni [a], Xiao Wu Peng [a,*]

[a] State Environmental Protection Key Laboratory of Environmental Pollution Health Risk Assessment, South China Institute of Environmental Sciences, Ministry of Ecology and Environment, Guangzhou 510535, China
[b] Nanning Center for Disease Control and Prevention, Nanning 530021, China
[c] Environment and Health Department, Shenzhen Center for Disease Control and Prevention, Shenzhen 518055, China

ARTICLE INFO

Edited by Bing Yan

Keywords:
Atmospheric fine particles
Human bronchial epithelial cells
Inflammatory response
CircRNA
CeRNA

ABSTRACT

Background: Studies have shown that fine particulate matter ($PM_{2.5}$) remains a significant problem in developing countries and plays a critical role in the onset and progression of respiratory illnesses. Circular RNAs (circRNAs) are involved in many pathophysiological processes,but their relationship to $PM_{2.5}$ pollution is largely unexplored.
Objectives: To elucidate the functional role of hsa_circ_0000992 in $PM_{2.5}$-induced inflammation in a human bronchial epithelial cell line (16HBE) and to clarify whether the competing endogenous RNA (ceRNA) mechanism is involved in the interrelationships between hsa_circ_0000992 and hsa-miR-936 and the inflammatory signaling pathways.
Methods: Detection of inflammatory factors in 16HBE cells exposed to $PM_{2.5}$ by RT-qPCR and ELISA.High throughput sequencing and bioinformatics analysis methods were used to screen circRNA.The bioinformatics analysis method western blotting and dual-luciferase reporter gene system were used to verify mechanisms associated with circRNA.
Results: $PM_{2.5}$ cause inflammation in the 16HBE cells. High throughput sequencing and RT-qPCR result revealed that the expression of hsa_circ_0000992 was markedly up-regulated in 16HBE exposed to $PM_{2.5}$. The binding sites between hsa_circ_0000992 and hsa-miR-936 was confirmed by dual-luciferase reporter gene system.Western blotting and RT-qPCR showed that hsa_circ_0000992 can interact with hsa-miR-936 to regulate AKT serine/threonine kinase 3(AKT3),thereby activating the PI3K/AKT pathway and ultimately promoting the expression of interleukin (IL)– 1β and IL-8.
Conclusion: $PM_{2.5}$ can induce the inflammatory response in 16HBE cells by activating the PI3K/AKT pathway. The expression of hsa_circ_0000992 increased when $PM_{2.5}$ stimulated 16HBE cells,and the circRNA could then regulate the inflammatory response.Hsa_circ_0000992 regulates the hsa-miR-936/AKT3 axis through the ceRNA mechanism,thereby activating the PI3K/AKT signaling pathway,increasing the expression of cellular inflammatory factors,and promoting $PM_{2.5}$-induced respiratory inflammation.

1. Introduction

Fine particulate matter ($PM_{2.5}$) refers to inhalable particles, with an aerodynamic diameters of 2.5 μm or smaller (≤2.5 μm). Due to its small size,$PM_{2.5}$ can remain suspended in air for a very long time and enters the human body through the inhalation route,where it can reach deep into the alveoli and finally enter the pulmonary circulatory system, resulting in a series of diseases related to cardiopulmonary dysfunction (Jo et al., 2018). Lancet Global Burden of Disease Study in 2015 reported that $PM_{2.5}$ pollution ranked seventh among all known health risk factors

* Corresponding author.
E-mail address: pengxiaowu@scies.org (X.W. Peng).
[1] These authors contributed equally to this work and should be considered co-first authors.

https://doi.org/10.1016/j.ecoenv.2023.115778
Received 23 April 2023; Received in revised form 27 November 2023; Accepted 29 November 2023
Available online 25 December 2023

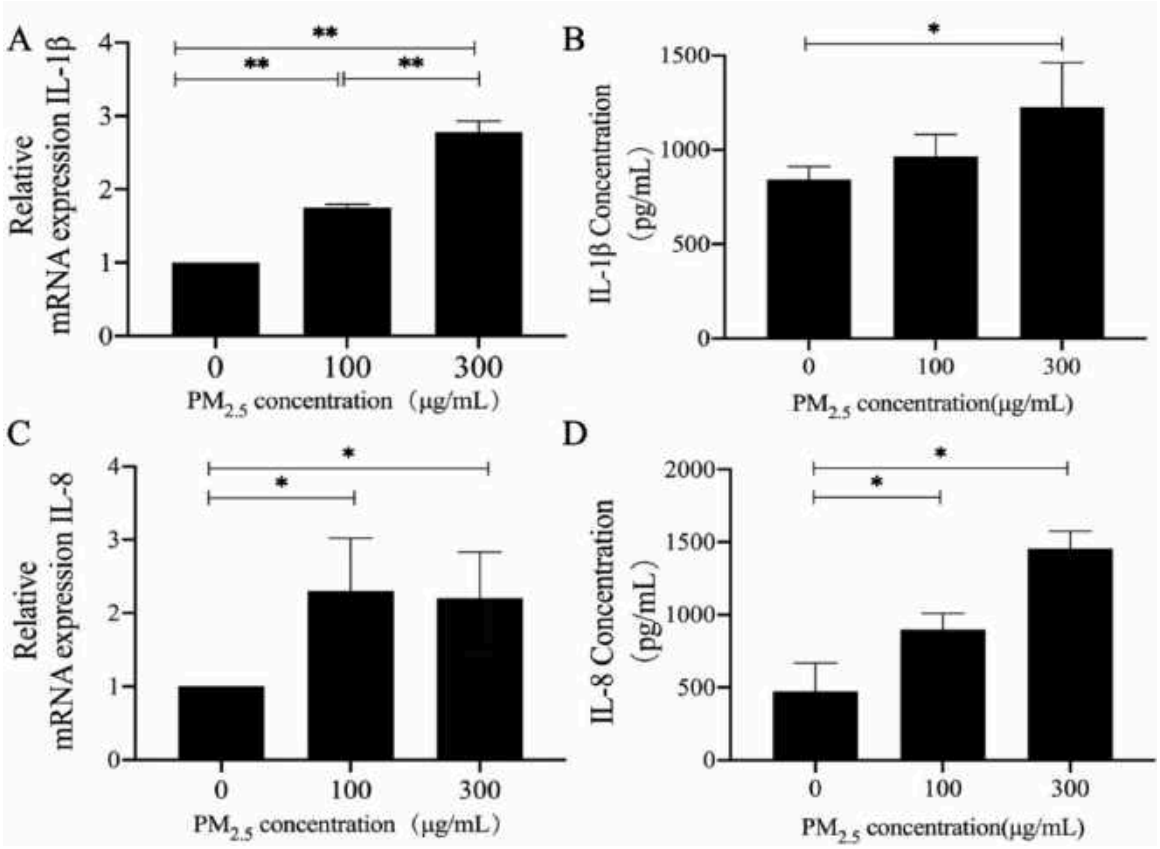

Fig. 1. Expression of inflammatory factors IL-1 β and IL-8 after 48 h of $PM_{2.5}$ stimulation. Note: A and C represent the expression levels of inflammatory cytokine transcripts detected by RT-qPCR assay; B and D represent the detection of inflammatory factor protein expression levels by ELISA assay; *$P < 0.05$, **$P < 0.01$.

(GBD Global Burden of Disease Study collaborators, 2015). Previous epidemiological studies addressed that populations living in an area with a high concentration of $PM_{2.5}$ for an extended period of time have increased morbidity and mortality rates associated with respiratory and cardiovascular diseases (Shang et al., 2013).

Multiple studies have determined that exposure to $PM_{2.5}$ can cause a variety of respiratory symptoms and disorders in humans,including impaired lung function, asthma, chronic obstructive pulmonary disease (COPD),and even lung cancer (Atkinson et al., 2014; Guo et al., 2018; Li et al., 2013). In addition, previous in vitro cell and in vivo animal toxicological studies indicated that $PM_{2.5}$ can induce various pathological responses, such as cytotoxicity,immune and inflammatory responses, oxidative stress,DNA damages,and gene mutations(Xian et al., 2019; Yang et al., 2019;Traboulsi et al., 2017). Polynomial studies showed that exposure to $PM_{2.5}$ can also affect gene expression (Zhou et al., 2015). However, the exact mechanisms through which $PM_{2.5}$ affects the respiratory system have not yet been fully understood. Additionally, the relationship between $PM_{2.5}$ induced epigenetic changes and their impact on cellular functions is still unknown.

Circular RNAs (circRNAs) are covalently closed single-stranded transcripts composed of many RNA species.These non-coding RNA sequences,which form a closed loop through covalent bonding of the 3′ and 5′ ends via backsplicing,have a high degree of tissue expression specificity in the eukaryotic transcriptome,RNA sequencing (RNA-SEQ) showed that circRNA expression was widely present in the detected cells and tissues, and more than 10% of the expressed genes could produce circRNA(Zhang et al., 2018). Previous reported on circRNAs in cancer (Bachmayr-Heyda et al., 2015), respiratory ailments (Yang et al., 2018; Li et al., 2018; Liu et al., 2017), and cardiovascular diseases (Burd et al., 2010). According to current reports on the function of circRNAs,its as competing endogenous RNAs (ceRNAs), acting as sponges of microRNAs (miRNAs) by competitively binding with them and modulating their functions,thereby regulating downstream target gene expression (Li et al., 2018).

CircRNA is widely involved in regulating physiological, pathological processes, and diseases by interacting with miRNA.Meanwhile, circRNA as a widely present non coding RNA with important regulatory functions in organisms,must be associated with other important biological macromolecules.Therefore,we propose a scientific hypothesis that the interaction between circRNA and MiRNA interaction plays an important role in the mechanism of $PM_{2.5}$ induced inflammatory response in 16HBE.In this study,we aimed to investigate whether the interaction between circRNA and miRNA is involved in $PM_{2.5}$ exposure induced respiratory inflammation.To achieve this,human bronchial epithelial cell line (16HBE) was exposed to $PM_{2.5}$ to construct a cellular inflammation model,and the effects on circRNA expression were examined using high-throughput sequencing techniques. A loss-of-function system was used to determine the functional role of the circRNA in $PM_{2.5}$-induced inflammation. Finally,the circRNA–miRNA–mRNA relationship was explored. We identified the hsa-circ_0000992,which was upregulated in 16HBE cell treated with $PM_{2.5}$. And we also speculated that hsa-circ_0000992 might be associated closely with the occurrence of inflammatory response by interacting hsa-miR-936 , and then regulating the AKT3 protein.

2. Materials and methods

2.1. $PM_{2.5}$ sample preparation

From January to February 2020, $PM_{2.5}$ samples were collected on the roof of an office building (Huangpu District, Guangzhou, China), using the TH1000C large flow sampler (Wuhan Tianhong, China) for 72 h of

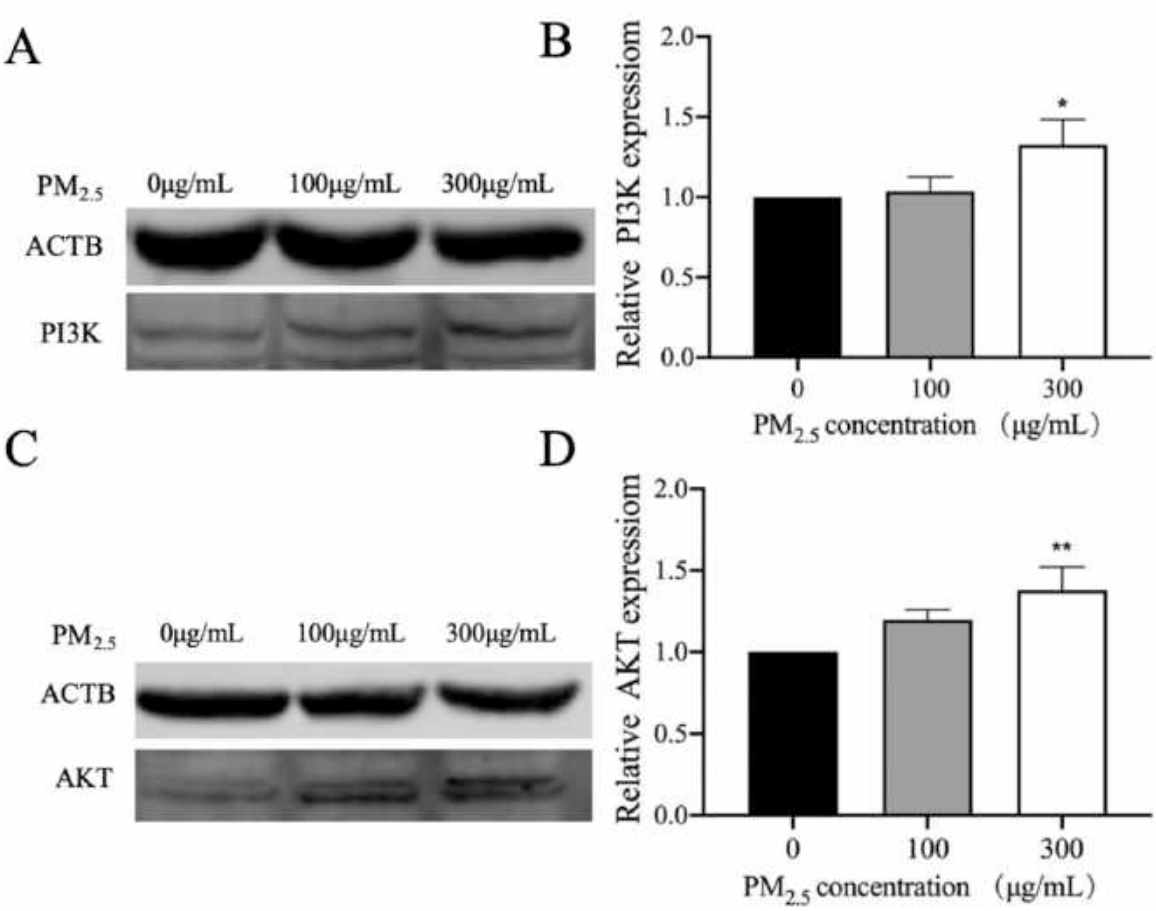

Fig. 2. Effect of $PM_{2.5}$ on the expression of PI3K/AKT signaling pathway proteins in 16HBE cells. Note: A and C indicate that $PM_{2.5}$ affects the expression of pathway proteins by western blotting; B and D indicate that $PM_{2.5}$ affects the expression of pathway proteins; compared with the 0 μg/mL $PM_{2.5}$ group, $^{*}P < 0.05$, $^{**}P < 0.01$.

continuous sampling at a flow rate of 1.05 m^3/min. The glass fiber membrane (1 ×1 cm^2) with the trapped $PM_{2.5}$ sample was added to a beaker containing ultrapure water, and an ultrasonic cleaner was then used to remove the entrapped particulate matter. The $PM_{2.5}$ suspension was divided into several glass conical flasks and stored overnight in a –80 °C refrigerator. The next day, the $PM_{2.5}$ suspension was dried using a vacuum freeze dryer.Finally, phosphate-buffered saline (Gibco, Thermo Fisher Scientific, Waltham, MA, USA) was used to prepare a high-concentration $PM_{2.5}$ stock solution,which was then sterilized in a high-pressure steam sterilizer and stored in a –20 °C refrigerator. To prepare different concentrations of the $PM_{2.5}$ suspension, the stock solution was diluted with culture medium.

2.2. Cell culture

The 16HBE cells were purchased from the ATCC cell bank.16HBE cells were cultured in complete keratinocyte medium (KM: 98% basal KM, 1% keratinocyte growth supplement, and 1% penicillin–streptomycin; ScienCell, Carlsbad, CA, USA) under a 5% CO_2 atmosphere at 37 °C.

2.3. Reverse transcription-quantitative polymerase chain reaction analysis

The quantitative analysis of target gene expression in the 16HBE cells was performed using the reverse transcription-quantitative polymerase chain reaction (RT-qPCR). In brief,16HBE cells (3.5 ×10^5/well) were seeded into the wells of a 6-well plate. After 24 h,the 16HBE cells were treated with various concentrations of the $PM_{2.5}$ suspension (0, 100, and 300 μg/mL). The $PM_{2.5}$ concentrations studied were determined on the basis of prior experimental results obtained by the research team and from published studies (Tan et al., 2020; Zhou et al., 2020). After 48 h of treatment, the 16HBE cells and supernatant were collected for the extraction of total RNA with the TRIzol reagent. After the RNA had been reverse transcribed into cDNA, qPCR was performed using the ABI StepOnePlus Real-Time PCR system (Applied Biosystems, Foster City, CA, USA). The expression level of the target gene was normalized to that of the beta-actin (ACTB) gene, and the relative expression level was calculated using the $2^{-\Delta\Delta CT}$ method. The gene primers used in this study were manufactured by Sangon Biotech (Shanghai, China) (Table S1).

2.4. Enzyme-linked immunosorbent assay

The 16HBE cells supernatant was collected for detection of protein levels via ELISA kits.Inflammatory factors protein levels were detected by IL-1β(CSB-E0805h,
CUSABIO) and IL-8(CSB-E0464,CUSABIO) ELISA kits.

2.5. High-throughput sequencing and data analysis

16HBE cells were exposed to various concentrations of the $PM_{2.5}$ suspension (0, 100, and 300 μg/mL) for 48 h and then collected and delivered to Guangzhou Geneseed Biological Technology Co., Ltd (Guangzhou, China) for high-throughput sequencing.

2.6. RNase R treatment

The $PM_{2.5}$ exposed 16HBE cells were divided into an RNase R group

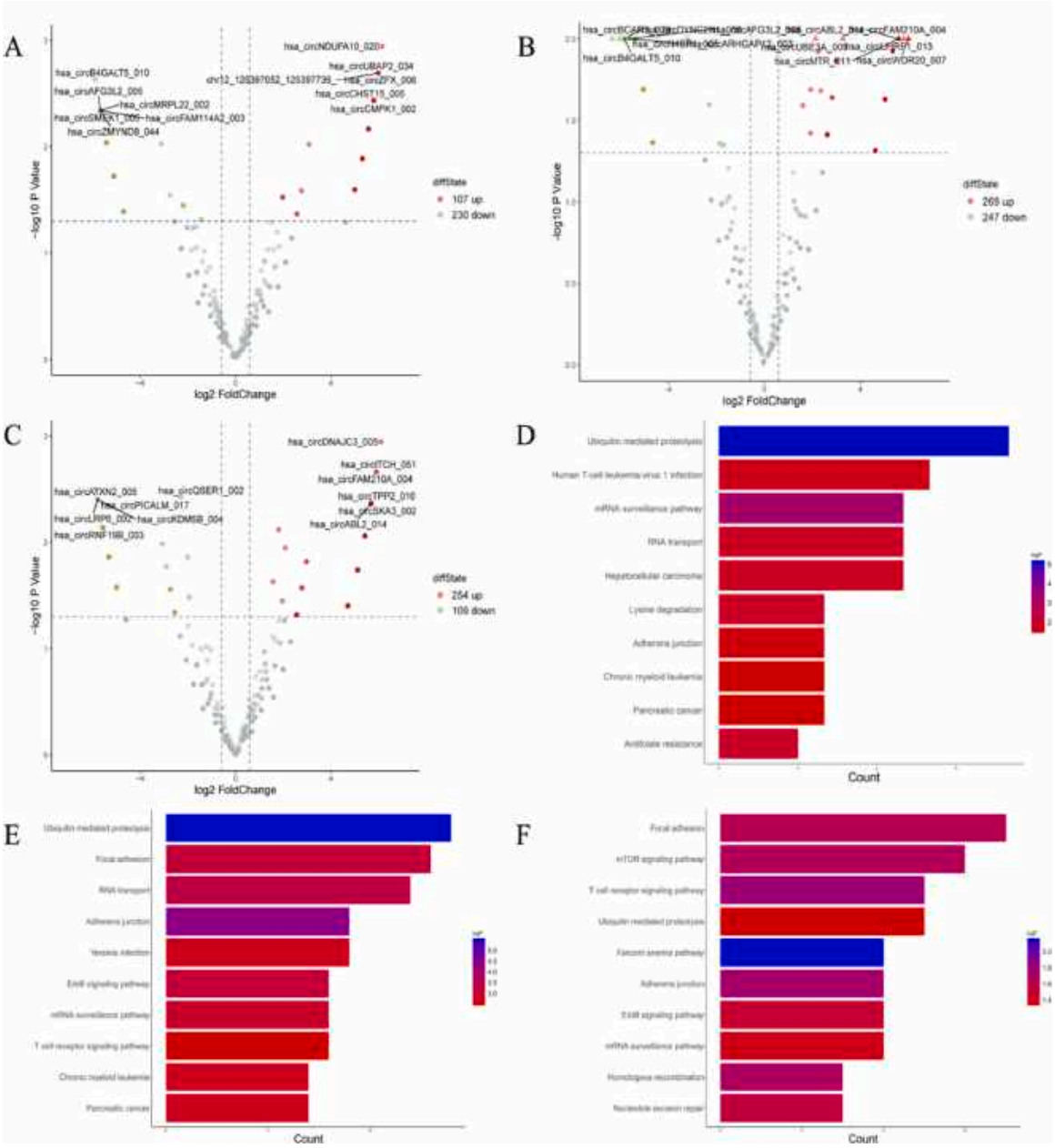

Fig. 3. CircRNA bioinformatics analysis. Note: A represents control group vs 100 μg/mL $PM_{2.5}$ exposure group; B represents control group vs 300 μg/mL $PM_{2.5}$ exposure group; C represents 100 vs 300 μg/mL $PM_{2.5}$ exposure group; above The graph is screened by the conditions of fold-change > 1.5 and $p < 0.05$, red represents up-regulated genes, green represents down-regulated genes, and gray represents genes with insignificant changes; D means control group vs 100 μg/mL $PM_{2.5}$ exposure group; E means control group vs 300 μg/mL $PM_{2.5}$ exposure group; F means 100 vs 300 μg/mL $PM_{2.5}$ exposure group.

(with RNase R enzyme treatment) and a control group (without RNase R treatment). Total RNA was then extracted from the cells and subjected to RT-qPCR as described in Section 2.2. The RNase R treatment was carried out according to the instructions of the manufacturer (Guangzhou Geneseed Biological Technology Co., Ltd).

2.7. Fluorescence in situ hybridization

Fluorescence in situ hybridization (FISH) was performed according to the instructions provided in the RNA FISH Kit (GenePharma, Shanghai, China). Finally, the cells were examined under an IX71 Inverted Research System Microscope (Olympus, Tokyo, Japan). The FISH probes were designed by Suzhou GenePharma Co., Ltd (Suzhou, China).

Hsa_circ_0000992 FISH probe sequence:
5′-GUGACAUA+UAGUUAGCC+UUUUGAUAAAC+UAUGG-3′CY3.
Hsa-miR-936 FISH probe sequence:
5′-CUGCGA+UUCCUCCC+UCUACUGU-3′FAM3.

2.8. Dual-luciferase reporter gene assay

16HBE cells were plated in 12well plates. Then, Lipofectamine 3000 was used to transfect the cells with luciferase plasmids carrying either the hsa_circ_0000992 wild type (WT) or mutant (MUT) or the hsa-miR-936 mimic or mimic-negative control (NC),according to the manufacturer's protocol.The dual-luciferase reporter gene plasmids carrying the hsa_circ_0000992 WT or MUT were designed and constructed by Guangzhou Ribo Biotechnology Co., Ltd (Guangzhou, China). The sequences are listed in Table S2. After 48 h transfection, relative luciferase activity was detected by using the Dual-Luciferase Reporter Assay

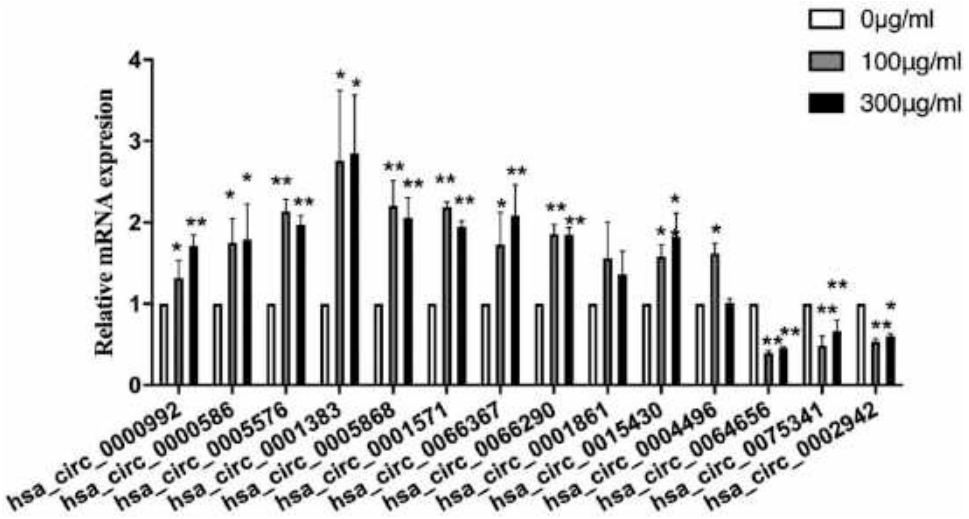

Fig. 4. Expression of circRNAs after 48 h of $PM_{2.5}$ exposure in 16HBE. Note: Compared with the 0 μg/mL $PM_{2.5}$ group, $^{*}P < 0.05$, $^{**}P < 0.01$.

System (E1910, Promega, Madison, WI, USA) and calculated through comparison against the firefly luciferase standard.

2.9. Cell transfection

16HBE were transfected by using transfection reagent Lipofectamine 3000 (Thermo Scientific,USA),according to the manufacturer's instructions,and the transfection efficiency was evaluated via RT-qPCR.All small interfering RNA (siRNA),miRNA mimic/inhibitor, and NC sequences were designed by Suzhou GenePharma Co., Ltd. The synthetic RNA oligonucleotide sequences are listed in Table S3.

2.10. Bioinformatics analysis

The miRanda,TargetScan7.2,and CircuLar RNA Interactome databases were used to predict miRNAs that may interact with circRNAs,and those related to inflammatory signaling pathways were screened. The miRanda software tool was used to predict the putative binding sequence of hsa_circ_0000992 and hsa-miR-936.

2.11. Western blot assay

Cells were lysed for western blot and immunoprecipitation protein analyses. The cell lysates contained 100 volumes of cell lysis buffer (Beyotime Biotechnology, Shanghai, China),1 vol of protease inhibitor (MedChemExpress, Monmouth Junstion, NJ, USA USA), and 1 vol of phenylmethylsulfonyl fluoride (Beyotime Biotechnology). The Pierce BCA Protein Assay Kit (NCI3225CH, Thermo Fisher Scientific) was used to quantify the total protein content.

Following established protocols,the denatured proteins were separated by sodium dodecyl sulfate-polyacrylamide gel electrophoresis on 10% gels (Beyotime Biotechnology) and then electrotransferred to polyvinylidene difluoride membranes (Millipore, Darmstadt, Germany). The membranes were soaked in a 5% nonfat milk powder blocking solution for 2 h and then incubated overnight with rabbit polyclonal primary antibodies to ACTB (CAT: 20346–1-AP, Proteintech, San Diego, CA, USA), PI3K (CAT: 20584–1-AP, Proteintech), AKT (CAT: 51077–1-AP, Proteintech), and AKT3 (CAT: 21641–1-AP, Proteintech) at 4 °C. After three washes with Tween 20-containing Tris-buffered saline,the membranes were incubated with IRDye800 CW-conjugated goat anti-rabbit IgG secondary antibodies (CAT: 926–32211, LI-COR, Lincoln, NB, USA) for 1 h in the dark. Finally, the blots were converted to images using ImageJ software and the protein bands were quantified using the Odyssey Sa Imaging System. ACTB was used as an internal reference to normalize the band density values of the target proteins.

2.12. Statistical analysis

GraphPad Prism 8.0 and SPSS 25.0 software were used for the statistical data analyses. All experiments were carried out in triplicate, and the results are reported as the mean and standard deviation.The t-test was used to compare two groups,and one-way analysis of variance was used to compare multiple groups.Differences with a P-value of less than 0.05 were considered statistically significant.

3. Results

3.1. Involvement of the PI3K/AKT signaling pathway in the $PM_{2.5}$ induced inflammatory response in 16HBE cells

After 48 h of exposure to $PM_{2.5}$ at concentrations of 0, 100, and 300 μg/mL, ELISA kits and RT-qPCR assays were used to detect changes in the IL-1β and IL-8 protein and mRNA levels in the 16HBE cells. Compared with the control group, the $PM_{2.5}$ groups had significantly higher mRNA and protein levels of IL-1β and IL-8 ($P < 0.05$) (Fig. 1).

The PI3K/AKT signaling system can induce inflammation by controlling the operation of major inflammatory signaling pathways as well as the function of leukocytes,which are critical to the inflammatory response.Western blotting was used to determine changes in the expression of proteins in the PI3K/AKT inflammatory signaling pathway after 16HBE cell exposure to 0, 100, and 300 μg/mL $PM_{2.5}$. The results showed that the PI3K ($P < 0.01$) and AKT ($P < 0.05$) protein levels in the 300 μg/mL $PM_{2.5}$ group were significantly higher than those in the control group, indicating that the PI3K/AKT signaling pathway is involved in $PM_{2.5}$-induced respiratory inflammation (Fig. 2).

3.2. $PM_{2.5}$ regulation of circRNA expression, and circRNA screening

After 48 h exposure to 0, 100, or 300 μg/mL $PM_{2.5}$,the 16HBE cells were subjected to high-throughput sequencing.CircRNA genes with a greater than 1.5 fold change in expression (with $P < 0.05$) were considered differentially expressed, and their related pathways were analyzed.Compared with their expression in the control group, 107circRNA genes were upregulated and 230 were downregulated in the 100 μg/mL $PM_{2.5}$ group, and 269 were upregulated and 247 were downregulated in the 300 μg/mL $PM_{2.5}$ group. Compared with their expression in the 100 μg/mL $PM_{2.5}$ group, 254 circRNA genes were upregulated and 109 were downregulated in the 300 μg/mL $PM_{2.5}$ group

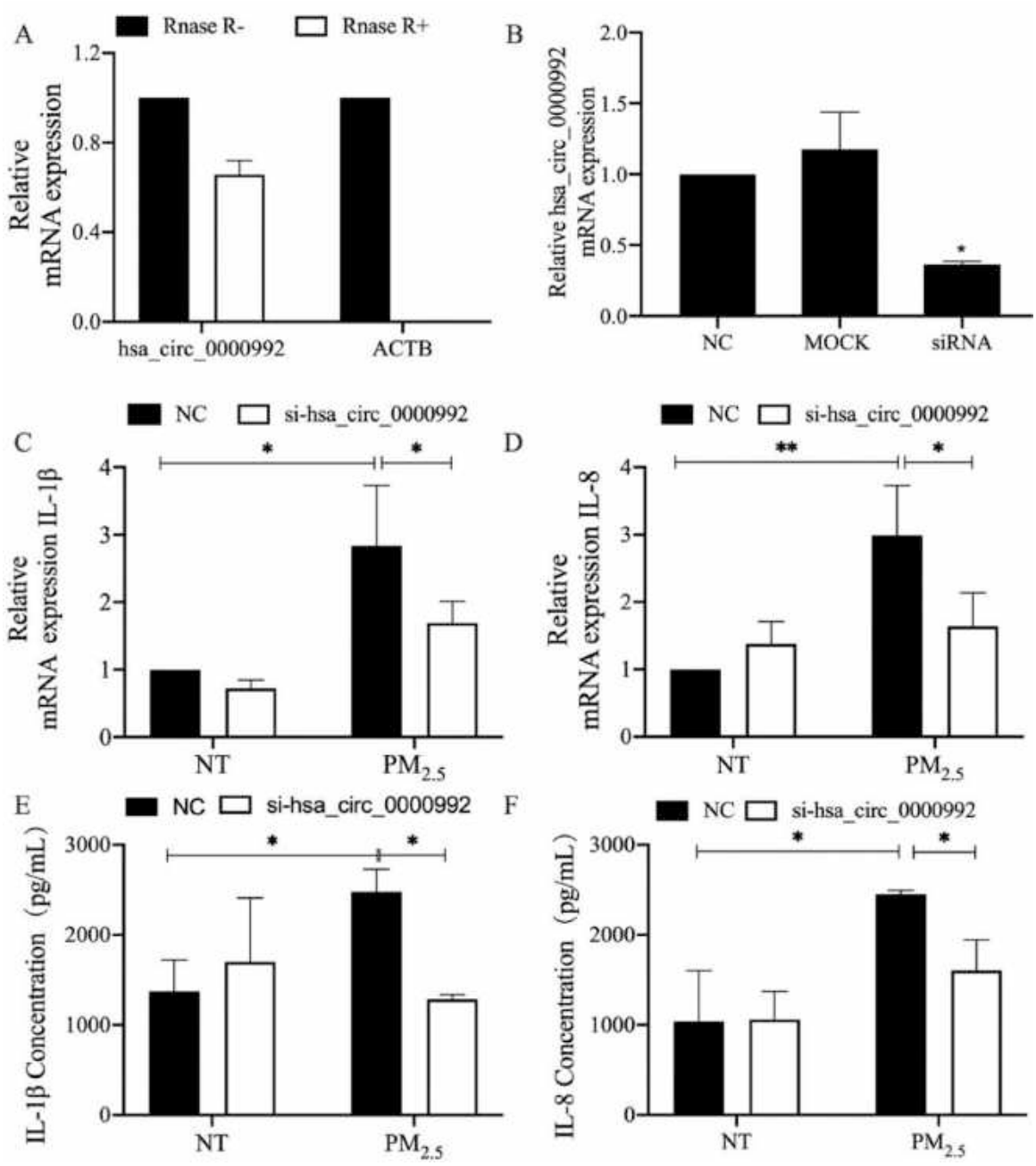

Fig. 5. Circular RNA hsa_circ_0000992 inflammation function verification. Note: A represent RNA stability identification of hsa_circ_0000992; B Knockdown efficiency of hsa_circ_0000992; C and D represent the expression levels of inflammatory factor transcripts detected by RT-qPCR; E and F represent the protein expression levels of inflammatory factors detected by ELISA assay; $^{*}P < 0.05$, $^{**}P < 0.01$.

(Fig. 3A–C). KEGG analysis of the differentially expressed circRNAs in each group revealed the pathways in which they were enriched (Fig. 3D–F).

The reliability of the high-throughput sequencing results was verified using the RT-qPCR assay.The results showed that the change trend in transcript levels of 14 circRNAs under different concentrations of $PM_{2.5}$ exposure was consistent with the sequencing results (Fig. 4). The circRNAs related to the inflammatory signaling pathway were screened out using bioinformatics analysis tools. The transcription level of hsa_circ_0000992 was significantly higher ($P < 0.05$) in the 100 and 300 μg/mL $PM_{2.5}$ groups than in the control group, indicating that $PM_{2.5}$ may induce the inflammatory response by regulating this particular circRNA (Fig. 4).

3.3. Verification of the circRNA nature of hsa_circ_0000992 and its inflammation related function

RNase R,which is a 3–5′ exonuclease, is a member of the Escherichia coli ribonucleotide reductase superfamily that can digest most linear RNA molecules. However, circRNAs are structurally stable and resistant to exonuclease.The RNA extracted from 16HBE cells was digested with RNase R and the expression of hsa_circ_0000992 and ACTB was then detected and quantitated using the RT-qPCR assay. The level of ACTB mRNA was significantly reduced in the cells, whereas that of hsa_circ_0000992 was only slightly decreased, confirming that hsa_circ_0000992 has the stability of typical circRNAs (Fig. 5A).

The 16HBE cells were transfected with siRNA (si-hsa_circ_0000992) to interfere with the expression of hsa_circ_0000992. After 48 h

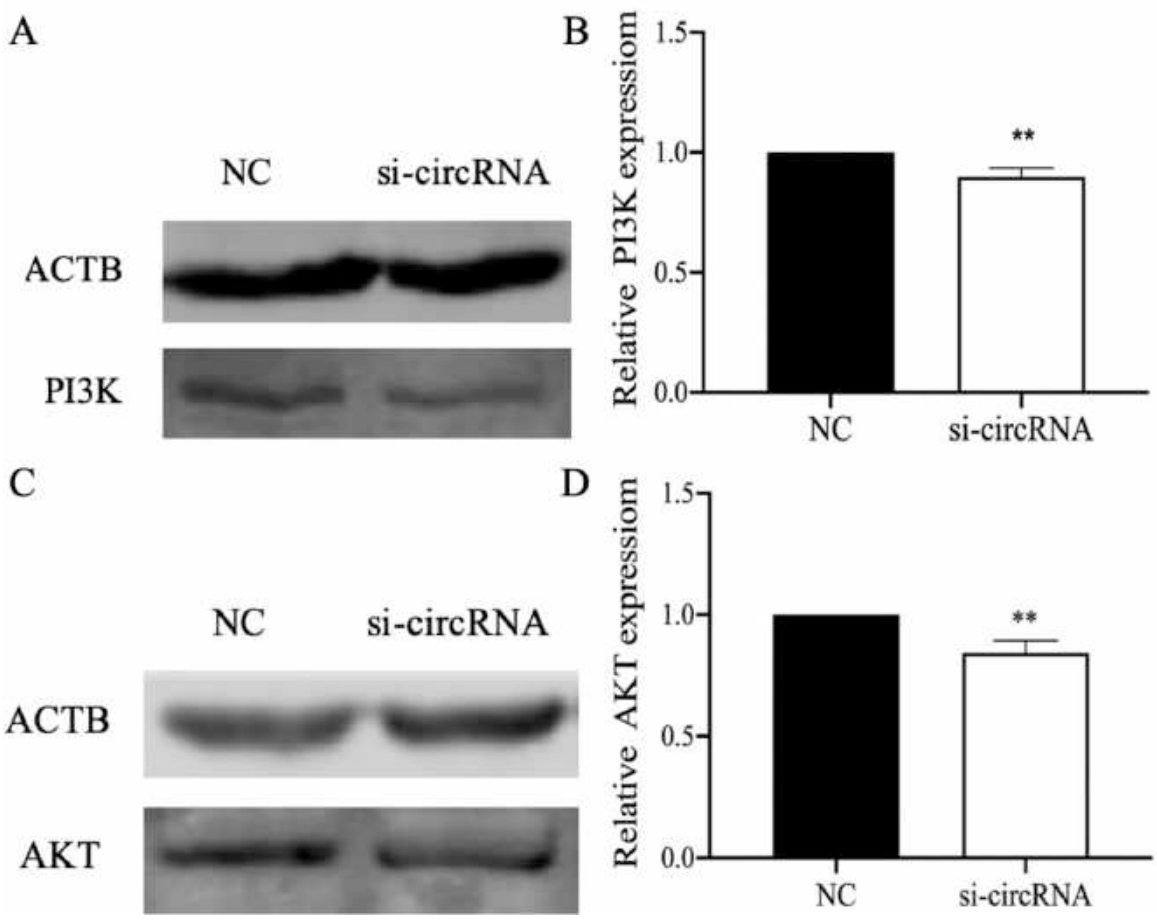

Fig. 6. Effect of knocking down hsa_circ_0000992 on the expression of PI3K/AKT signaling pathway proteins in 16HBE cells. Note:; A and C indicate the expression of pathway proteins after knockdown of hsa_circ_0000992 detected by western blotting; B and D indicate the results of grayscale analysis of the expression of pathway proteins after knockdown of hsa_circ_0000992; compared with the NC group, * *P < 0.01.

transfection, the hsa_circ_0000992 expression level was confirmed using the RT-qPCR assay. There was no statistically significant difference in hsa_circ_0000992 expression between the MOCK and NC groups. However, the transcriptional level of hsa_circ_0000992 was significantly lower in the si-hsa_circ_0000992 group than in the NC group ($P < 0.05$), and the transfection efficiency was approximately 70% (Fig. 5B). This indicated that si-hsa_circ_0000992 had effectively interfered with the expression of hsa_circ_0000992 and thus could be used for the subsequent interference experiments.

Next, 16HBE cells were transfected with si-NC or si-hsa_circ_0000992 for 5 h and then treated with complete KM (control group) or $PM_{2.5}$ (300 mg/mL). After 48 h, the protein and mRNA levels of IL-lβ and IL-8 were determined.Compared with the mRNA and protein levels of IL-lβ and IL-8 in the NC group,the levels were significantly reduced in the 300 μg/mL $PM_{2.5}$-exposed cells transfected with si-hsa_circ_0000992 ($P < 0.05$) (Fig. 5C–F),indicating that hsa_circ_0000992 plays a role in promoting the inflammatory response induced by $PM_{2.5}$.

3.4. Influence of hsa_circ_0000992 on the PI3K/AKT signaling pathway

The western blot assay was used to determine the levels of PI3K and AKT in 16HBE cells in which hsa_circ_0000992 had been knocked down. The levels of both proteins were significantly lower ($P < 0.01$) in the hsa_circ_0000992 knockdown group than in the control group (Fig. 6), suggesting that the knockdown of hsa_circ_0000992 in 16HBE cells can inhibit the activation of the PI3K/AKT inflammatory signaling pathway and thereby regulate the inflammatory response.

3.5. Bioinformatics prediction analysis of miRNAs that may bind to hsa_circ_0000992

The bioinformatics analysis tools miRanda,TargetScan7.2,and Circular RNA Interactome were used to predict miRNAs that may bind to hsa_circ_0000992. Among the miRNAs identified, 70 were predicted by miRanda, 668 were predicted by TargetScan7.2,and 36 were predicted by Circular RNA Interactome. All three software tools predicted that hsa-miR-936 and hsa-miR-127–5 P could bind to hsa_circ_0000992. Therefore, these two miRNAs were selected for the subsequent experiments (Fig. 7).

3.6. Changes in hsa-miR-936 expression in 16HBE cells after $PM_{2.5}$ exposure and hsa_circ_0000992 knockdown

The transcript levels of hsa-miR-936 in the 100 and 300 μg/mL $PM_{2.5}$ groups were significantly lower ($P < 0.05$) than that in the control group (Fig. 8A). By contrast, those of hsa-miR-127–5p were higher (Fig. 8B), but the difference was not statistically significant. Compared with that in the NC group, the transcript level of hsa-miR-936 was increased after hsa_circ_0000992 had been knocked down in the 16HBE cells ($P < 0.05$) (Fig. 8C). By contrast, the transcript level of hsa-miR-127–5p was unchanged (Fig. 8D). These results suggested that hsa_circ_0000992 and hsa-miR-936 had a mutual regulatory relationship.

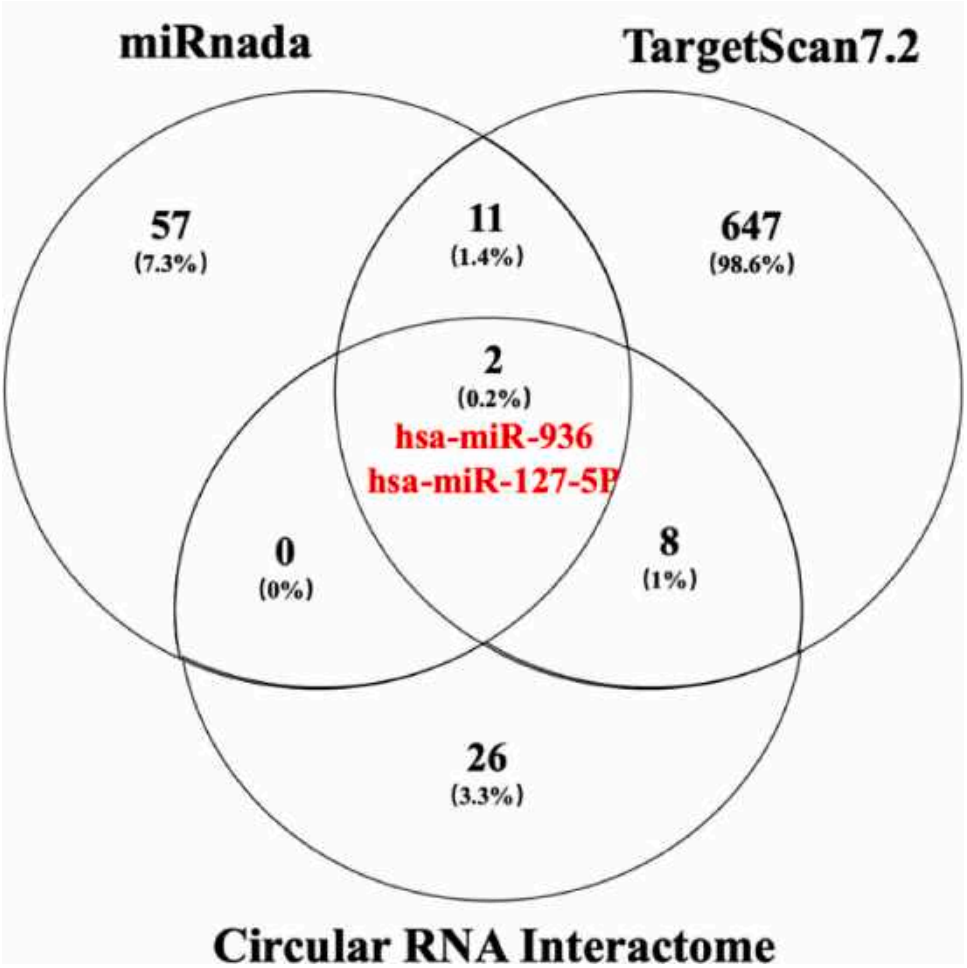

Fig. 7. Venn diagram of bioinformatics software prediction result.

3.7. Effects of hsa-miR-936 mimics and inhibitors on cellular inflammatory factors

Hsa-miR-936 inhibitors and mimics can respectively inhibit and enhance hsa-miR-936 expression in cells (Fig. 9A). Therefore, 16HBE cells were transfected with either an hsa-miR-936 inhibitor or mimic and then exposed to 300 μg/mL $PM_{2.5}$ for 48 h.Subsequently, the cells were collected to determine changes in their expression of cellular inflammatory factors. In the $PM_{2.5}$-exposed cells, the mRNA level of the IL-1β gene was significantly lower in the hsa-miR-936 mimic group than in the NC group ($P < 0.05$) (Fig. 9B). By contrast, the mRNA and protein levels of IL-1β and IL-8 were higher in the hsa-miR-936 inhibitor group ($P < 0.05$) (Fig. 9C–F). These results indicate that hsa-miR-936 plays a role in suppressing the $PM_{2.5}$-induced inflammatory response.

3.8. Effect of hsa_circ_0000992 on hsa-miR-936 in 16HBE cells

Because the localization of RNA in cells is related to their mode of action, a FISH study was performed to determine the subcellular location of hsa_circ_0000992 and hsa-miR-936 in the 16HBE cells. Hsa_circ_0000992 and hsa-miR-936 were revealed to be expressed in the nucleus and cytoplasm (Fig. 10A), suggesting that they may both play a regulatory role in the $PM_{2.5}$-induced inflammatory response of 16HBE cells through the ceRNA mechanism.

The binding site between hsa_circ_0000992 and hsa-miR-936 was predicted using miRanda. The results showed that hsa-miR-936 and hsa_circ_0000992 may have a binding site with a binding score of 152 points (Fig. 10B).

The dual-luciferase reporter gene assay was performed to confirm the binding site of hsa_circ_0000992 and hsa-miR-936. After co-transfection of the hsa-miR-936 mimic or NC plasmids with the hsa_circ_0000992 WT or MUT reporter genes into 16HBE cells,changes in fluorescence due to luciferase activity were detected. In the hsa_circ_0000992-WT cells, the relative luciferase activity in the hsa-miR-936 mimic group was considerably lower ($P < 0.05$) than that in the NC group. By contrast, in the hsa_circ_0000992-MUT cells,there was no significant change in the relative luciferase activity between the hsa-miR-936 mimic and NC groups (Fig. 10C). These results indicate that hsa_circ_0000992 acts as a sponge to bind hsa-miR-936 through the binding site predicted by miRanda.

3.9. Verification of the roles of hsa_circ_0000992 and hsa-miR-936 in regulating inflammatory responses

To verify the mutual regulatory activity between hsa_circ_0000992 and hsa-miR-936, the expression of inflammatory factors in 16HBE cells co-transfected with these circRNA and miRNA sequences was determined using RT-qPCR and ELISA.Compared with the NC group, the NC $PM_{2.5}$-exposed group expressed significantly higher levels of IL-1β and IL-8 ($P < 0.01$). Compared with the $PM_{2.5}$ exposure-alone group, the $PM_{2.5}$ +hsa-miR-936 inhibitor group expressed significantly higher mRNA and protein levels of IL-1β and IL-8 ($P < 0.05$), but re-transfection with si-hsa_circ_0000992 reversed this trend (Fig. 11). These results indicate that hsa_circ_0000992 directly targets hsa-miR-936 to regulate the inflammatory response.

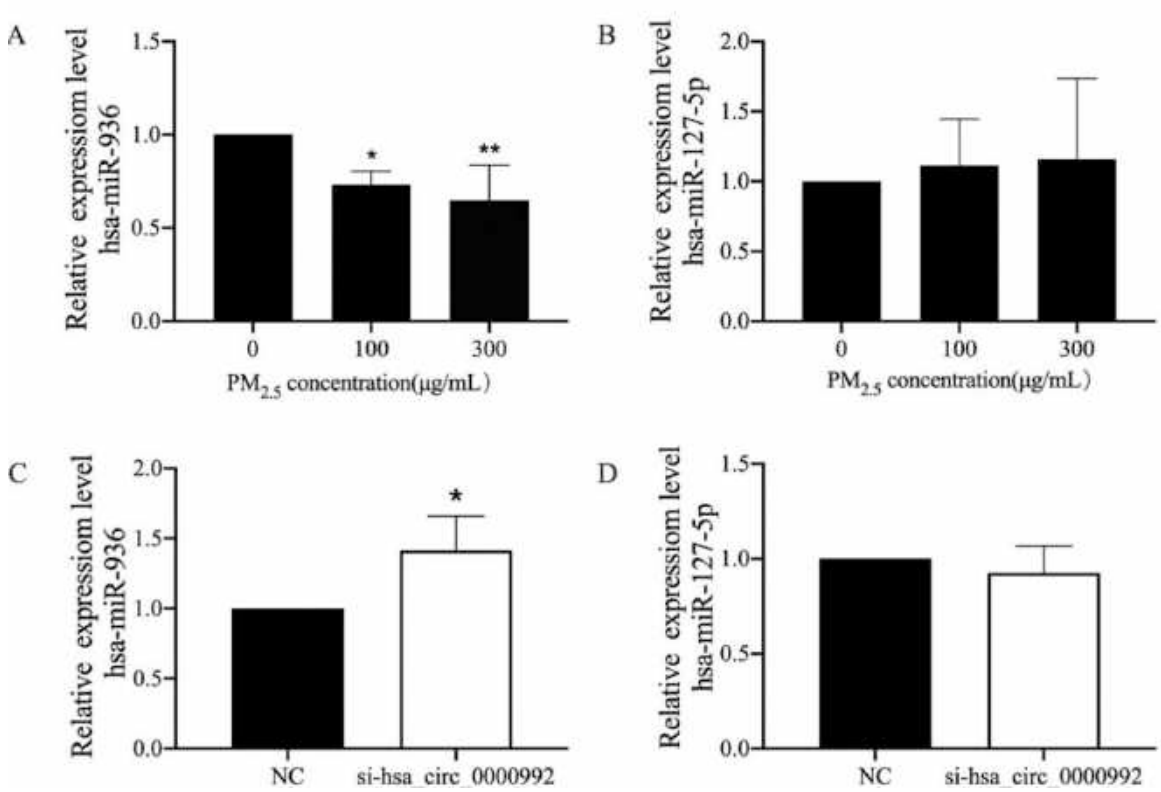

Fig. 8. The expression levels of miRNA after $PM_{2.5}$ stimulation and knocking down of hsa_circ_0000992 in 16HBE. Note: A and B represented miRNA expression after $PM_{2.5}$ treatment in 16HBE; C and D represented miRNA expression after knocking down of hsa_circ_0000992 in 16hbe; compared with the NC group, $^{*}P < 0.05$, $^{**}P < 0.01$.

3.10. Construction of the circRNA–miRNA–mRNA network

The TargetScan7.2, miRanda, and CircuLar RNA Interactome databases were used to predict the downstream target genes of hsa-miR-936, and a total of 1861 mRNAs were discovered after intersecting the results (Fig. 12A). KEGG analysis of these 1861 genes revealed that they were enriched in inflammation-related pathways, including the PI3K/AKT, MAPK,Ras,FOXO, TNF, T-cell receptor,Jak/STAT, Toll-like receptor, B-cell receptor, and NFκB signaling pathways (Fig. 12B).Fig. 12C depicts the network map of hsa_circ_0000992, hsa-miR-936, and their downstream mRNAs in inflammation-related pathways, as constructed using Cytoscape software.

3.11. Regulatory relationship between hsa_circ_0000992 and hsa-miR-936 and the PI3K/AKT pathway

According to the western blot results, the expression of PI3K protein was inhibited in the si-hsa_circ_0000992+ hsa-miR-936 inhibitor group, unlike that in the hsa-miR-936 inhibitor group ($P < 0.05$) (Fig. 13A–B). Transfection of the hsa-miR-936 inhibitor markedly increased AKT protein expression relative to the level in the NC group, whereas concurrent hsa_circ_0000992 knockdown completely reversed this phenomenon (i.e., AKT protein expression was inhibited) ($P < 0.05$) (Fig. 13C–D). The results suggest that hsa_circ_0000992 directly targets hsa-miR-936 to regulate activation of the PI3K/AKT inflammatory signaling pathway.

3.12. Verification of the regulatory role of hsa-miR-936 on the expression of the downstream target gene AKT3

Through bioinformatics software prediction and KEGG pathway analysis, AKT3 was discovered to be not only a downstream target gene of hsa-miR-936 but also a key protein in the PI3K/AKT signaling pathway.In 16HBE cells transfected with the hsa-miR-936 inhibitor, the mRNA and protein levels of AKT3 were significantly enhanced ($P < 0.01$), indicating that hsa-miR-936 regulates AKT3 expression to control the activation of the PI3K/AKT signaling pathway (Fig. 14).

4. Discussion

In recent years, with the frequent occurrence of smog worldwide, especially in China,the pollution of fine particulate matter has become an environmental health problem that the word is keenly concerned about. According to the WHO report in 2016, the global death toll due to air pollution was approximately 4.2 million, with that related to $PM_{2.5}$ being the most prevalent (Wang et al., 2021). The main components of $PM_{2.5}$ include metals and metalloids (lead, manganese, aluminum, etc.), water-soluble inorganic ions (SO_4^{2-}, NH_4^+, NO_3^-, etc.), chemical components (organic carbon, carbon black, dust), and organic polycyclic aromatic hydrocarbons (Qiao et al., 2014; Qin et al., 2020; Zhu et al., 2019). $PM_{2.5}$ comes from a wide range of sources, including dust from the natural environment, fuel (fossil, biomass, coal, etc.) combustion, and transportation emissions from human activities (Khan et al., 2021; Xu et al., 2021; Zhang et al., 2015; Zhao et al., 2021). Because $PM_{2.5}$ has a small particle size and can remain suspended in air, it easily adsorbs toxic substances, such as heavy metals and microorganisms, and can be transported over long distances, resulting in large-scale air pollution. $PM_{2.5}$ can enter the deep respiratory tract, pass through the blood gas barrier, and enter the circulatory system, causing bodily harm and disorders of the respiratory, cardiovascular, and neurological systems (Mukherjee and Agrawal, 2018; Xing et al., 2016). $PM_{2.5}$ can reach the bronchi and alveoli of the lungs through the respiratory tract, causing inflammation of the respiratory system and the release of inflammatory factors, thereby leading to a series of respiratory diseases. Despite that

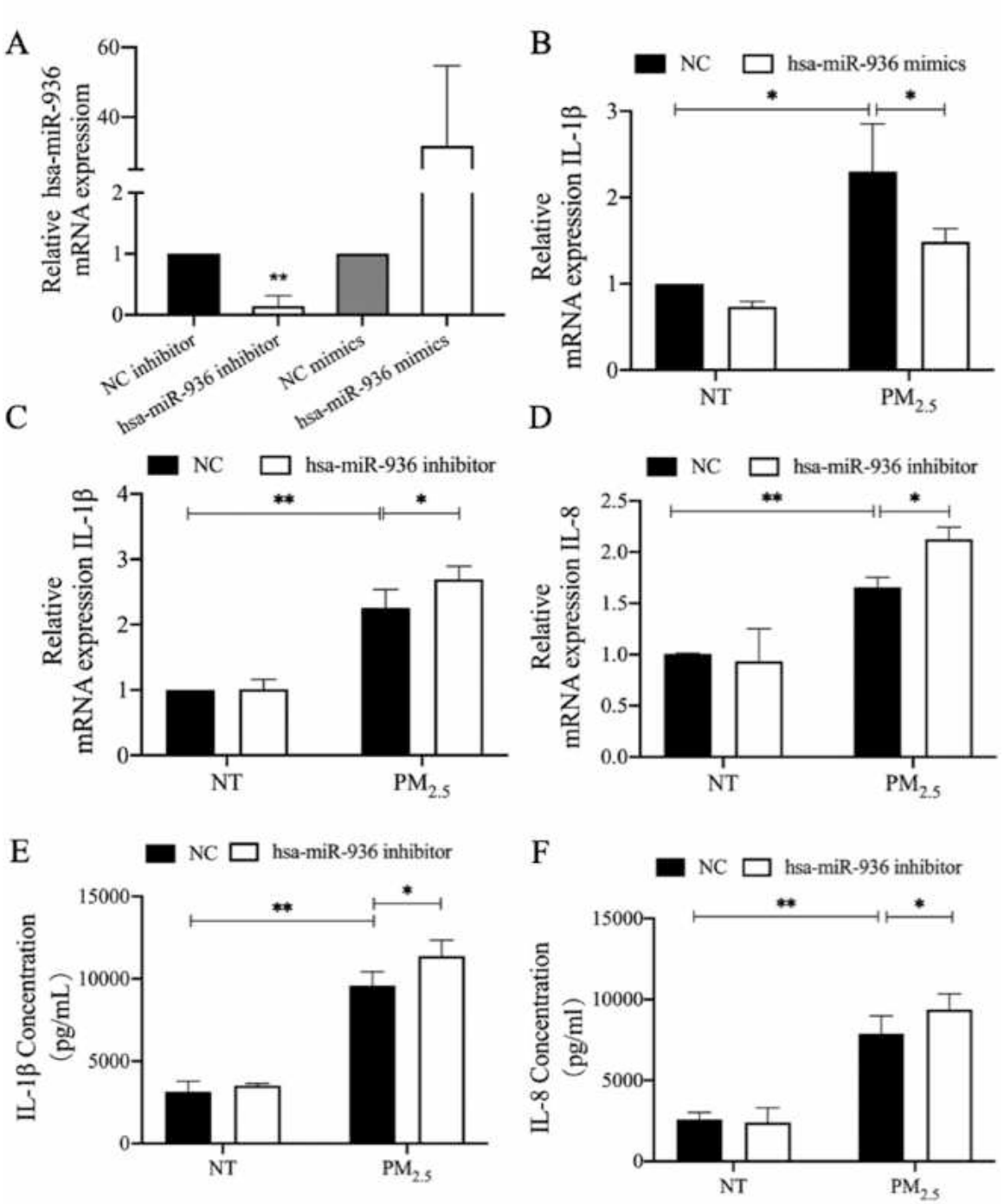

Fig. 9. Hsa-miR-936 inflammation function verification. Note: A indicates the transcript expression level of hsa-miR-936 detected by RT-qPCR experiment; B and D indicates the transcript expression level of inflammatory factors detected by RT-qPCR experiment; E and F indicate the protein expression level of inflammatory factors detected by ELISA experiment; $^{*}P < 0.05$, $^{**}P < 0.01$.

the first line of defense against the dangers of air pollution is the respiratory system, the mechanism by which $PM_{2.5}$ enters the human respiratory tract and causes respiratory diseases remains unclear. With the increasing development of science and technology, the study of toxicological mechanisms has shifted from a macroscopic to a microscopic perspective, and epigenetic research has received keen attention from scholars. However, there are few published studies on the mechanism of $PM_{2.5}$ induced respiratory diseases from the viewpoint of epigenetics.

$PM_{2.5}$ can promote pulmonary inflammation, and peripheral blood mononuclear cells greatly increase the release of inflammatory factors such as IL-1β, IL-8, and IL-10 (Xian et al., 2019). Li et al. (2020) observed that $PM_{2.5}$ exposure boosted the expression of IL-1β and IL-18 in the lung tissue of normal mice and COPD model mice. Another study found that $PM_{2.5}$ from underground garages had a substantial effect on mouse levels of IL-4, TNF-α, and TGF-β1, which can lead to lung injury (Yang et al., 2019). The expression levels of inflammatory (IL-1β) and cyclooxygenase 2) and oxidative stress (heme oxygenase 1) genes were considerably upregulated in mouse macrophages exposed to $PM_{2.5}$ (Bekki et al., 2016). According to Longhin et al. (2018), $PM_{2.5}$ increases the mRNA and protein levels of IL-6 and IL-8, resulting in the development of inflammatory responses. IL-1β, a member of the IL-1 family of cytokines, triggers inflammation through the IL-1 receptor family and

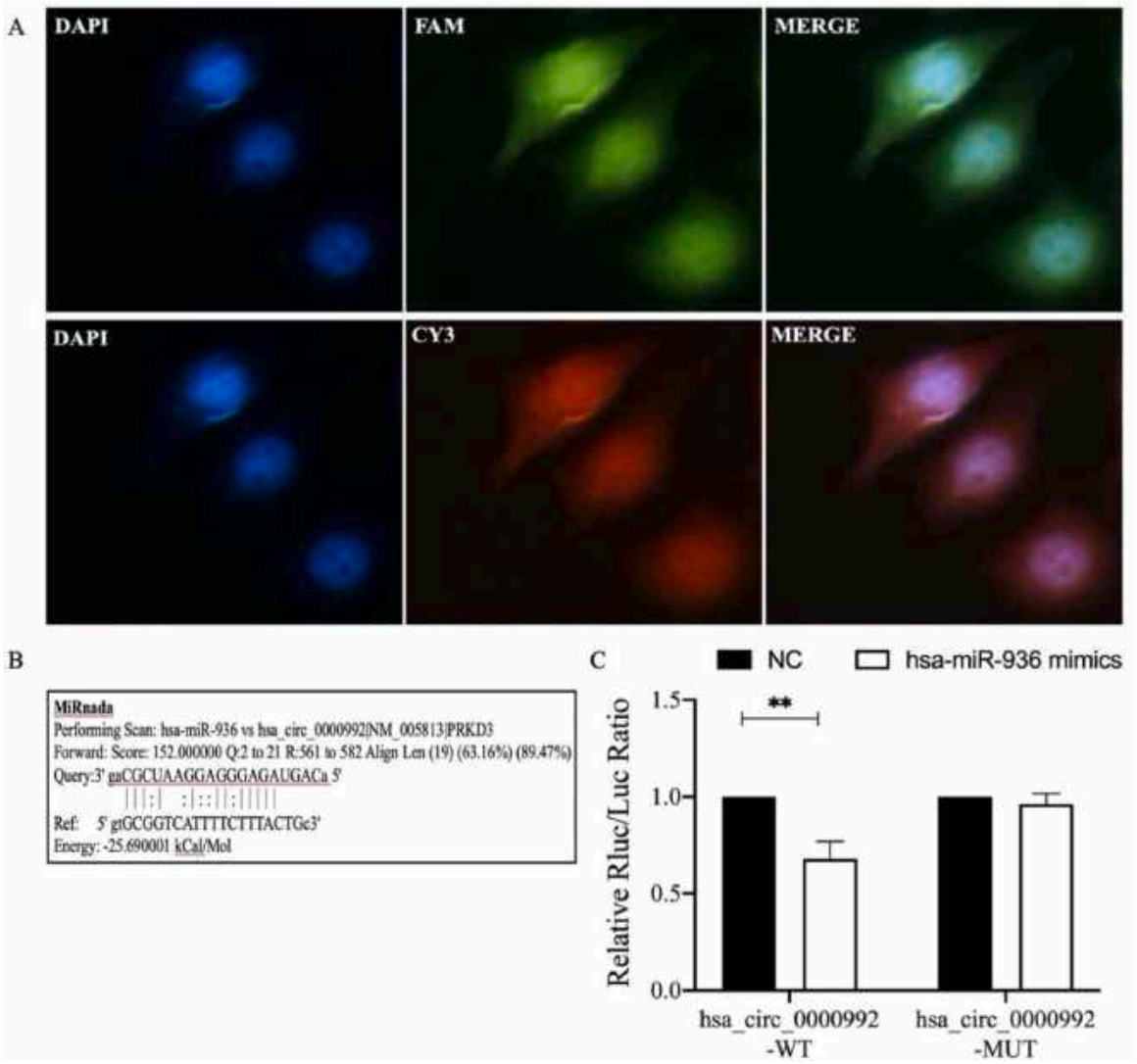

Fig. 10. hsa_circ_0000992 acted as a sponge for hsa-miR-936 in 16HBE cells. Note: A represented FISH experiment diagram. blue: DAPI nuclear staining, green: FAM-labeled hsa-miR-936 probe, red: CY3-labeled hsa_circ_0000992 probe; B represented MiRnada analysis and prediction of hsa_circ_0000992 and hsa-miR-936 binding sites; C represented Luciferase reporter gene confirms the existence of binding sites between hsa_circ_0000992 and hsa-miR-936; $^{**}p < 0.01$.

plays an important role in the development of inflammation, making it useful as an indicator for differentiating the occurrence of the inflammatory response (Dinarello, 2018). Additionally, Li et al. (2021) have verified that IL-8 is strongly associated with inflammatory signaling pathways and plays a critical role in the onset and progression of airway inflammation. As a result, we chose IL-1β and IL-8 as the indicators of an inflammatory response in our present study. On the basis of a literature review and preliminary research findings, we collected $PM_{2.5}$ samples at a specific location in Guangzhou (Tan et al., 2020; Zhou et al., 2020) and exposed 16HBE cells to 0, 100, and 300 μg/mL $PM_{2.5}$ concentrations for 48 h. Consequently, we found that $PM_{2.5}$ caused the mRNA and protein expression levels of IL-1β and IL-8 to increase in the 16HBE cells, indicating that it could increase the expression of cellular inflammatory factors and cause the inflammatory response. Hence, it was verified that the cellular inflammation model had been successfully constructed.

Previous studies have demonstrated that the PI3K/AKT signaling pathway can enhance the development of inflammation by modulating important inflammatory signaling pathways as well as the function of leukocytes critical to the inflammatory response (Yeung et al., 2018). $PM_{2.5}$ stimulation can activate the PI3K/AKT signaling pathway and induce cell inflammation and apoptosis (Han and Zhuang, 2021). Using a COPD mouse model established through $PM_{2.5}$ exposure, Zhang et al. (2020) found that PI3K inhibitors could decrease cell autophagy, enhance apoptosis in alveolar epithelial cells, and lower the expression of the PI3K, p-AKT, and p-mTOR proteins. The findings of our study suggest that the PI3K/AKT signaling pathway is involved in the development of $PM_{2.5}$-induced respiratory inflammation, because the PI3K and AKT protein levels were significantly higher in the 300 μg/mL $PM_{2.5}$ group than in the control group.

CircRNAs, which are a class of non-linear and endogenous non-coding RNA molecules that are ubiquitous in eukaryotic cells, are mainly produced by intron or exon sequences, transcribed by RNA polymerase II, form a closed-loop structure by reverse splicing, and resistant to exonuclease degradation (Guo et al., 2014; Memczak et al., 2013; Salzman et al., 2013). CircRNAs are currently a hot topic in epigenetic research and play a pivotal role in the development of diseases related to gene regulation. In this study, 16HBE cells were exposed to 0, 100, or 300 μg/mL $PM_{2.5}$ for 48 h, following which the expression profiles of circRNAs in the various treatment groups were examined using high-throughput sequencing and their biological functions were analyzed.CircRNA genes were considered to be differentially expressed if the change in their expression was 1.5 fold greater than that in the control group ($P < 0.05$). The 100 μg/mL $PM_{2.5}$ group had 107 upregulated and 230 downregulated circRNAs,whereas the 300 μg/mL $PM_{2.5}$

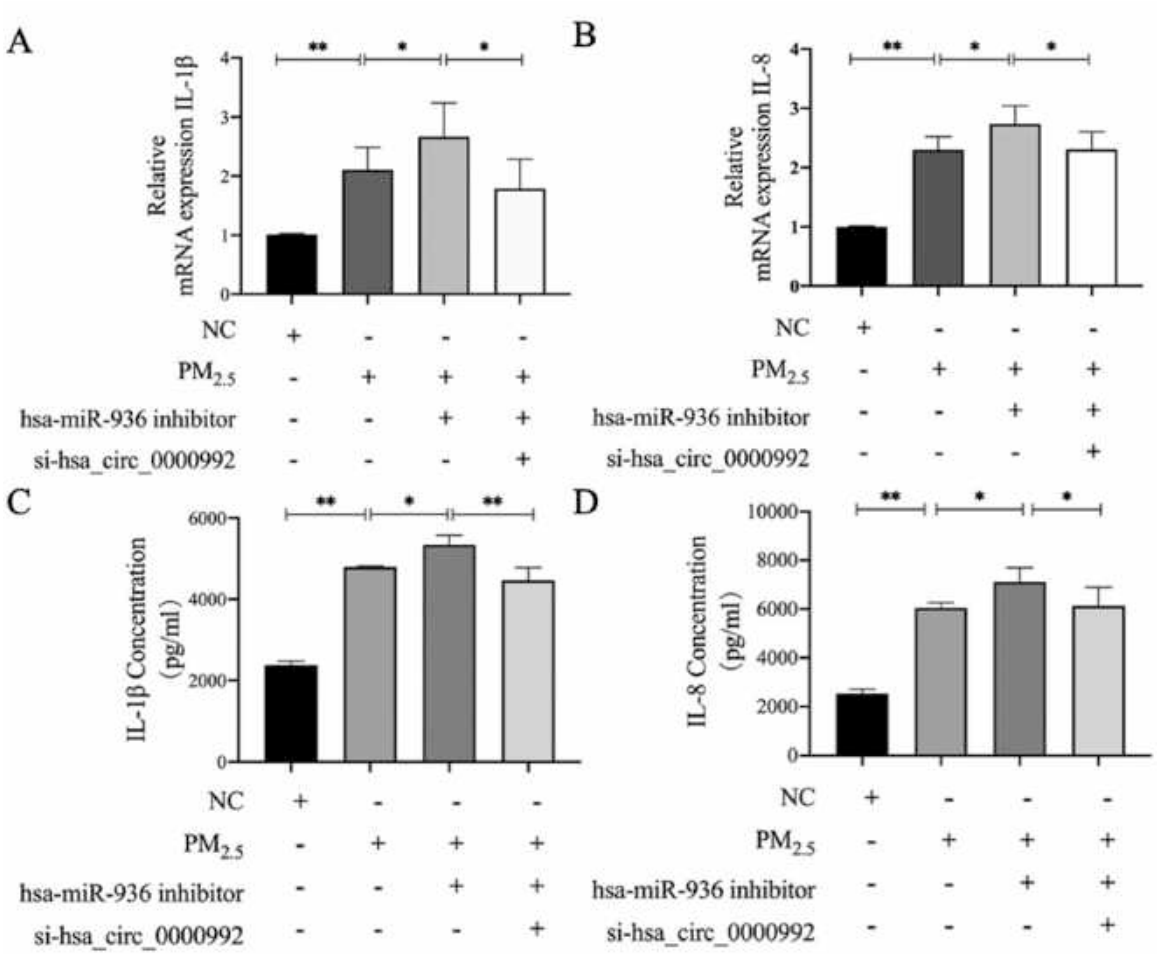

Fig. 11. Expression of inflammatory factors IL-1 β and IL-8 after co-transfection si-hsa_circ_0000992 and hsa-miR-936 inhibitor. Note: A and B represent the expression levels of inflammatory cytokine transcripts detected by RT-qPCR assay; C and D represent the protein expression levels of inflammatory factors detected by ELISA assay; $*P < 0.05$, $**P < 0.01$.

group had 269 upregulated and 247 downregulated circRNAs,relative to the control group circRNA levels. Moreover, in the 300 μg/mL $PM_{2.5}$ group,254 circRNAs were upregulated and 109 were downregulated relative to the levels in the 100 μg/mL $PM_{2.5}$ group.The circRNAs related to inflammatory signaling pathways were screened out using bioinformatics tools, and their expression change trend in the $PM_{2.5}$-exposed cells was verified through RT-qPCR analysis.We found that the transcription level of hsa_circ_0000992 increased with increase in the $PM_{2.5}$ exposure dose. Using RNase R, we verified that hsa_circ_0000992 has the characteristic circRNA resistance to delinearization enzymes. Therefore, hsa_circ_0000992 was selected for the subsequent experiments.

Ghosal et al. (2013) have created a comprehensive database of circRNAs (Circ2Traits) that may be related to diseases and traits. Many studies have reported on circRNAs play an indispensable role in the development of the $PM_{2.5}$ induced inflammatory response. Yang et al. (2018) found that circRNA ZC3H4 is related to the inflammatory cascade caused by silica phagocytosis of lung cells and participates in the activation of macrophages in lung tissue. Liu et al. (2017) showed that mechanical stress-related circRNAs are involved in chondrocyte extracellular matrix degradation and regulate the expression of TNF-α, thereby affecting the progression of osteoarthritis. Li et al. (2020) study showed that the knockdown of circBbs9 alleviated $PM_{2.5}$-induced respiratory inflammation by inactivating the inflammasome and inhibiting IL-1β and IL-18 in cells. According to Jia et al. (2020), exposure of human bronchial epithelial BEAS-2B cells to $PM_{2.5}$ increases the expression of IL-6 and IL-8 while decreasing that of circ_406961, the latter of which is a circRNA that would normally inhibit the $PM_{2.5}$-induced inflammatory response by interacting with interleukin enhancer-binding factor 2(ILF2) and inhibiting the activation of the STAT3/JNK pathway. We used the transient transfection technique to knock down the expression of hsa_circ_0000992 in 16HBE cells to determine its role in controlling the $PM_{2.5}$-induced inflammatory response. The results showed that hsa_circ_0000992 was successfully knocked down in cells, with a knockdown efficiency of approximately 70%. The mRNA and protein levels of IL-1β and IL-8 were lower in the si-hsa_circ_0000992 group than in the NC group. Moreover, the PI3K and AKT protein levels were significantly decreased in the si-hsa_circ_0000992 group. These results indicate that hsa_circ_0000992 promotes the inflammatory response in 16HBE cells by activating the PI3K/AKT inflammatory signaling pathway and boosting the production of IL-1 and IL-8.

The ceRNA mechanism employed by circRNAs currently accounts for the majority of their biological functions, physiological processes, and pathogenic mechanisms. CircRNAs possess miRNA response elements, which allow them to bind competitively to miRNAs and influence the latter's gene silencing activity and thereby regulate the expression of downstream target genes. Numerous studies have demonstrated that the ceRNA mechanism of circRNAs and miRNAs is crucial for the emergence and progression of many diseases and disorders. For example, circRNA CDR1as regulates nervous system function by binding to miR-7 (which has 63 conserved circRNA-binding sites) in neuronal cells (Memczak et al., 2013). This mechanism of competitive binding of circRNAs to miRNAs is expected to bring about a breakthrough in gene diagnosis and treatment. Therefore, we focused on exploring whether

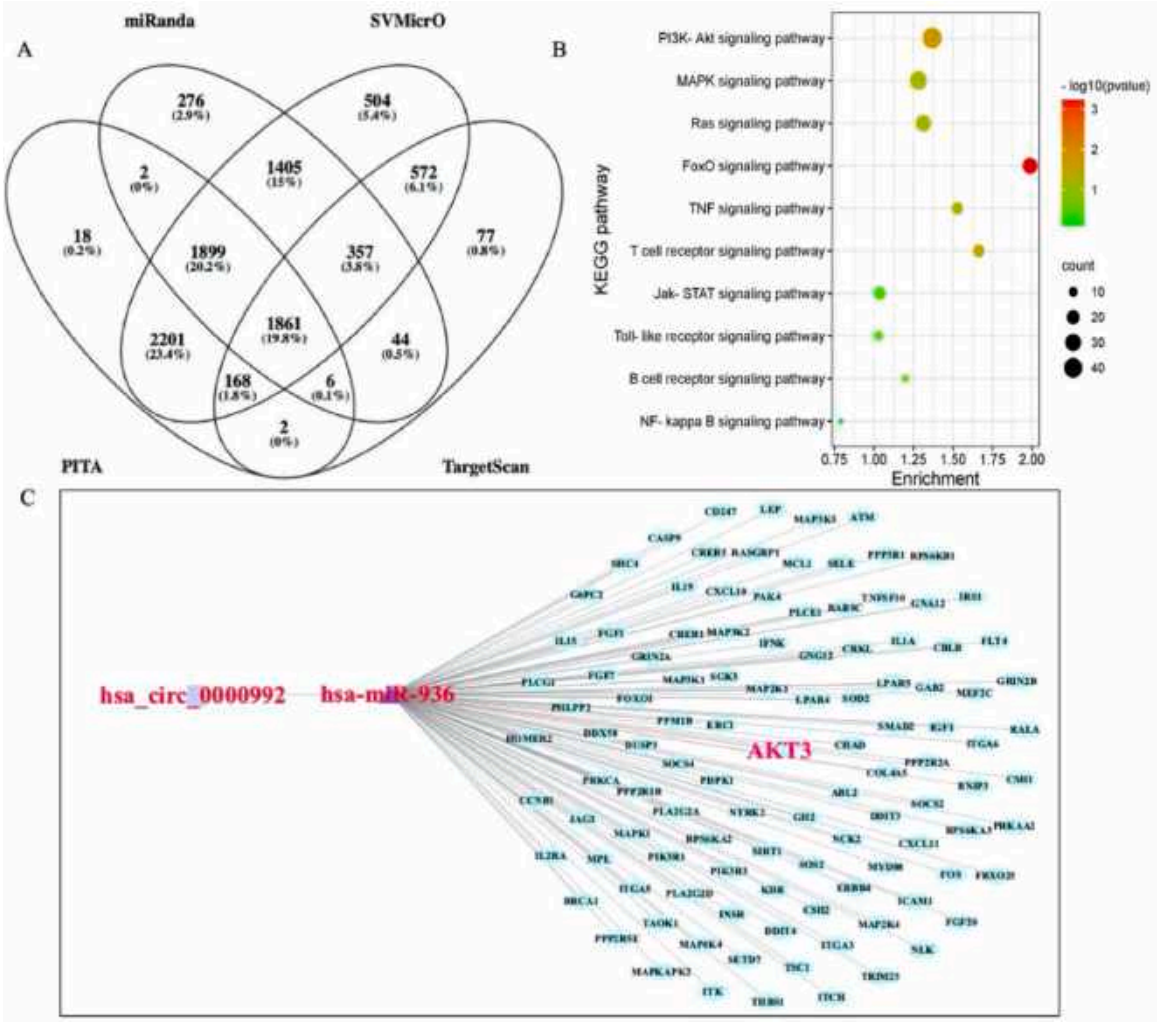

Fig. 12. circRNA-miRNA bioinformatics analysis. Note: A represented Venn diagram of miRNA downstream target gene predicting by Bioinformatics software; B represented the top 10 KEGG signaling pathways of inflammation-related; C represented hsa_circ_0000992-hsa-miR-936-mRNA co-expression network.

hsa_circ_0000992 adsorbs miRNA via the ceRNA mechanism and thereby regulates the mRNA expression of downstream target genes. In this study, three bioinformatics analysis software predicted the binding of hsa_circ_0000992 to hsa-miR-936 and hsa-miR-127–5 P. The RT-qPCR results showed that the expression of hsa-miR-936 transcript decreased with increasing exposure to $PM_{2.5}$, whereas the concurrent knockdown of hsa_circ_0000992 increased the expression level significantly. These results suggest that there is a great possibility of mutual regulation between hsa_circ_0000992 and hsa-miR-936. Further FISH experiments showed that hsa_circ_0000992 and hsa-miR-936 were localized in the cytoplasm and nucleus in 16HBE cells. The binding site of hsa_circ_0000992 and hsa-miR-936 was predicted and confirmed using miRanda software and the dual-luciferase reporter gene assay, respectively. Since the ceRNA mechanism mainly functions in the cytoplasm, we speculate that hsa_circ_0000992 can act as a ceRNA to adsorb hsa-miR-936, thereby regulating the expression of downstream target genes.

MiR-936 is linked to the proliferation, cell cycle progression, and invasion of non-small cell lung cancer, where its expression has been shown to be considerably downregulated in tissue of patients with this disease (Zhou and Tao, 2018). The miR-936/G protein-coupled receptor 78 (GPR78) axis has been established as a diagnostic and therapeutic target for laryngeal squamous cell carcinoma (Lin et al., 2020). Although these studies suggested that hsa-miR-936 is associated with respiratory diseases,its relationship with the respiratory inflammatory response was not clarified. In this study,we found that the mRNA level of IL-1β in the $PM_{2.5}$-treated cells transfected with the hsa-miR-936 mimic was considerably lower than that in the NC group. Additionally, in $PM_{2.5}$-treated cells, the mRNA and protein levels of IL-1β and IL-8 were significantly higher in the hsa-miR-936 inhibitor group than in the NC group. These results suggest that hsa-miR-936 reduces the inflammatory response induced by $PM_{2.5}$.

Researchers have found that both lncRpa and circRar1 can bind to miR-671 through the ceRNA mechanism and induce the upregulation of apoptosis-related factors p38 and caspase-8 at both the mRNA and protein levels (Nan et al., 2017). One study showed that circRNA_09505 acted as a sponge of miR-6089 through the ceRNA mechanism in macrophages and promoted the development of inflammation through the production of TNF-α, IL-12, and IL-6, which is regulated by the miR-6089/AKT1/NFκB axis (Yang et al., 2020). To verify whether mutual regulation between hsa_circ_0000992 and hsa-miR-936 exists, the expression of inflammatory factors was detected in 16HBE cells co-transfected with these circRNA and miRNA sequences and their inhibitors. Compared with the $PM_{2.5}$ group, the $PM_{2.5}$ + hsa-miR-936 inhibitor group had significantly higher mRNA and protein levels of IL-1β and IL-8, and this result was reversed through re-transfection of the cells with si-hsa_circ_0000992. Additionally, the expression of PI3K was inhibited in the cells co-transfected with si-hsa_circ_0000992 and the hsa-miR-936 inhibitor, and AKT expression was markedly higher in cells transfected with the hsa-miR-936 inhibitor than in the NC group (in

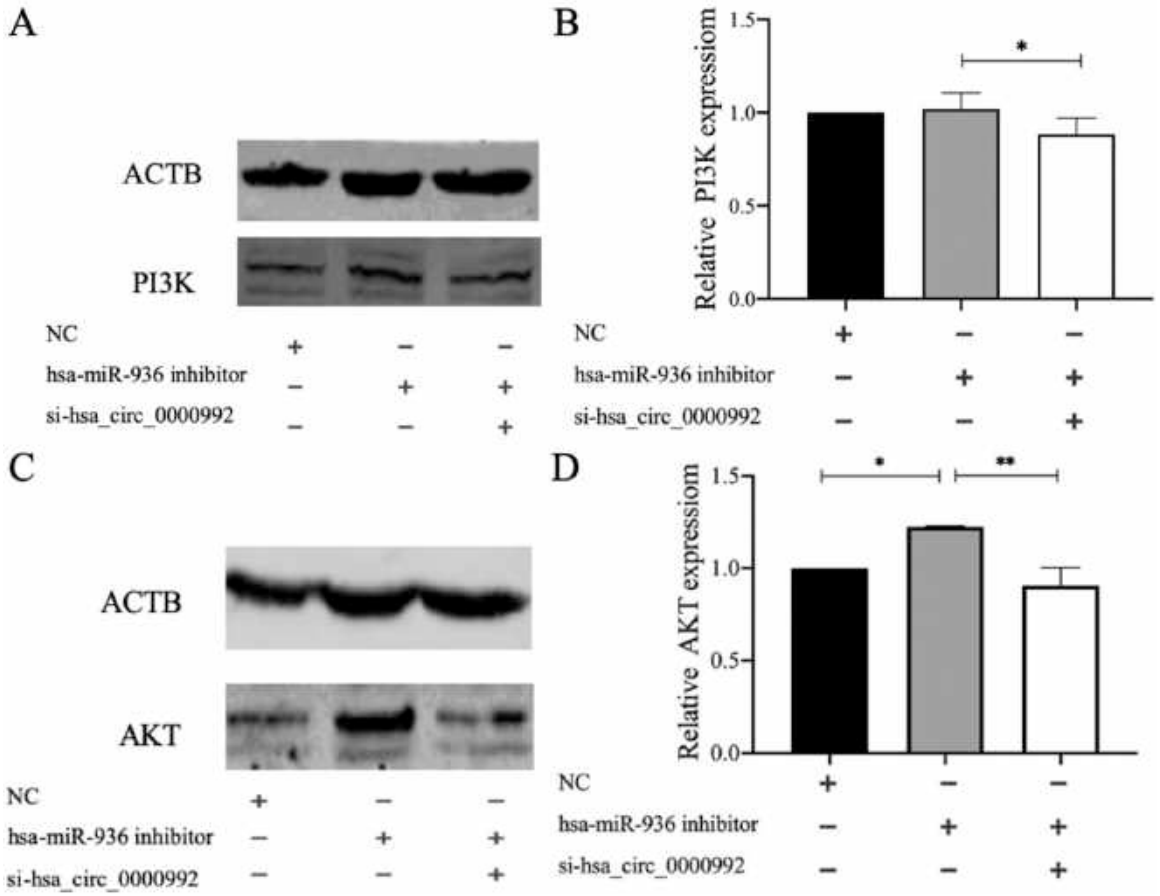

Fig. 13. The expression of PI3K/AKT signaling pathway proteins in 16HBE cells after the Transfection of si-hsa_circ_0000992 and hsa-miR-936 inhibitor on 16HBE. Note: A and C represent the expression of the pathway protein detected by western blotting; B and D represent the grayscale analysis result of the protein expression of the pathway.

which AKT expression was inhibited). We concluded that hsa_circ_0000992 targets hsa-miR-936 directly to regulate the PI3K/AKT inflammatory signaling pathway and the inflammatory response.

AKT is a 60 kDa serine/threonine kinase that is mainly involved in the PI3K/AKT signaling pathway and the regulation of downstream proteins of biological processes such as cell proliferation, migration, metabolism, and angiogenesis (Revathidevi and Munirajan, 2019). AKT can be divided into three subtypes (AKT1, AKT2, and AKT3), among which AKT3 is positively correlated with the inflammatory response and macrophage activation (Ding et al., 2017; Gu et al., 2020). A previous study found that silencing the expression of AKT3, which is a downstream target gene of miR-150, can suppress the levels of IL-1β, IL-6, and TNF-α (Yao et al., 2021). In this study, we found that AKT3 was not only a downstream target gene of hsa-miR-936 but also an important protein in the PI3K/AKT signaling pathway, as its mRNA and protein expression levels were significantly increased in 16HBE cells transfected with the hsa-miR-936 inhibitor. This implies that hsa-miR-936 may influence PI3K/AKT signaling pathway activity by influencing AKT3 expression. Based on our results and the findings of previous studies, blocking the expression of AKT3 may be an effective strategy for inhibiting the development of inflammatory responses.

In conclusion, this study confirms that $PM_{2.5}$ induces an inflammatory response in 16HBE cells. Hsa_circ_0000992 adsorbs hsa-miR-936 via the ceRNA mechanism, promotes the release of AKT3 and activation of the PI3K/AKT signaling pathway, and thereby regulates the development of the inflammatory response in $PM_{2.5}$-exposed 16HBE cells (Fig. 15), hsa_circ_0000992 might be a possible target for therapeutic intervention after $PM_{2.5}$ exposure. However, there are some limitations in this study, our research lacks in vivo experiments. Therefore, animal experiments will be carried out for further verification.Our verification of the involvement of the ceRNA mechanism in the hsa_circ_0000992 regulation of hsa-miR-936 and the inflammatory response of respiratory epithelial cells to $PM_{2.5}$ offers a scientific foundation for future research on the diagnosis, screening, and treatment of respiratory illnesses induced by air pollution.

CRediT authorship contribution statement

Li JingLin: Data curation, Methodology, Writing – original draft. **Tan Yi:** Conceptualization, Data curation, Formal analysis, Methodology, Writing – original draft, Writing – review & editing. **Wang QiuLing:** Methodology, Writing – original draft. **Li CaiXia:** Data curation. **Hong JinChang:** Data curation, Investigation. **Wang Hong Jie:** Data curation, Formal analysis, Resources. **Wu Yi:** Conceptualization, Data curation. **Ni DeChun:** Writing – review & editing. **Peng XiaoWu:** Funding acquisition, Project administration, Resources.

Declaration of Competing Interest

We declare that we do not have any commercial or associative interest that represents a conflict of interest in connection with the work submitted.

Data Availability

No data was used for the research described in the article.

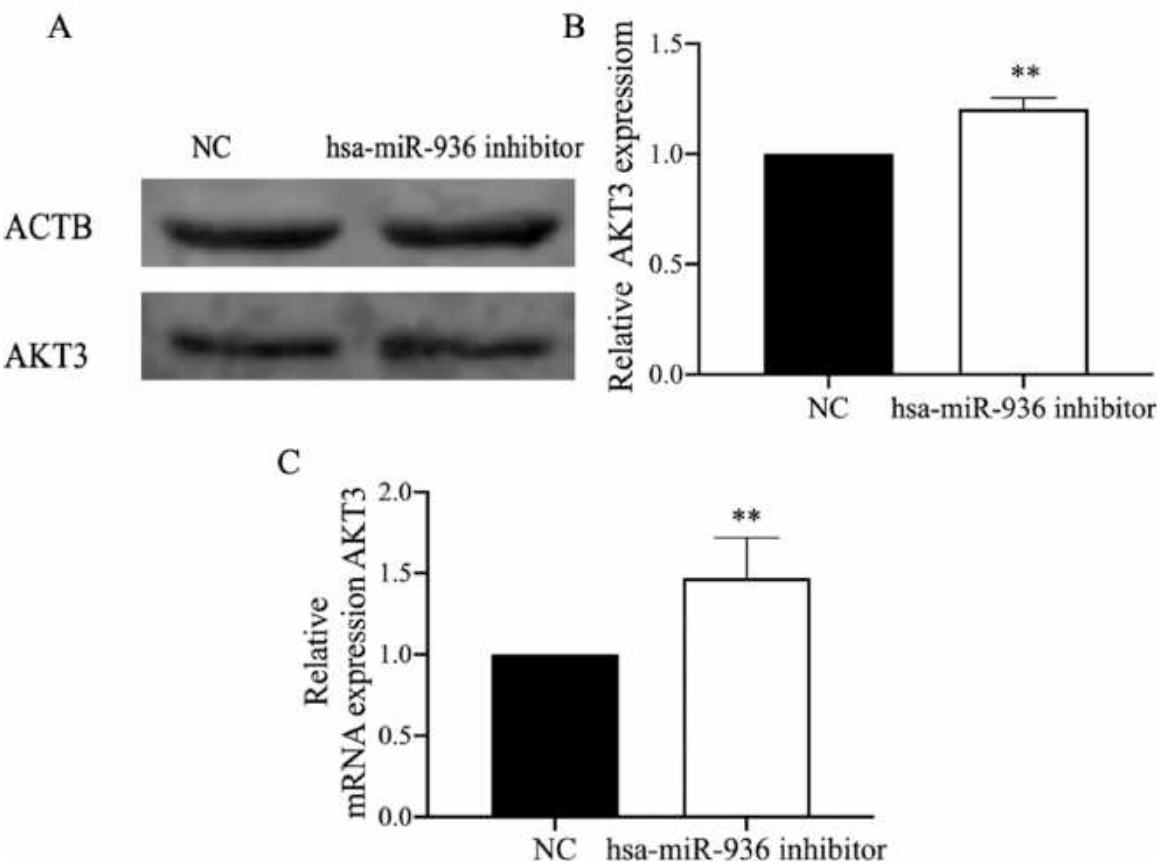

Fig. 14. The expression of AKT3 after hsa-miR-936 inhibitor transfection in 16HBE cells. Note: A represents the expression of the pathway protein detected by western blotting; B represents the grayscale analysis result of the protein expression of the pathway; C represents the expression level of the transcript detected by RT-qPCR; * * $P < 0.01$.

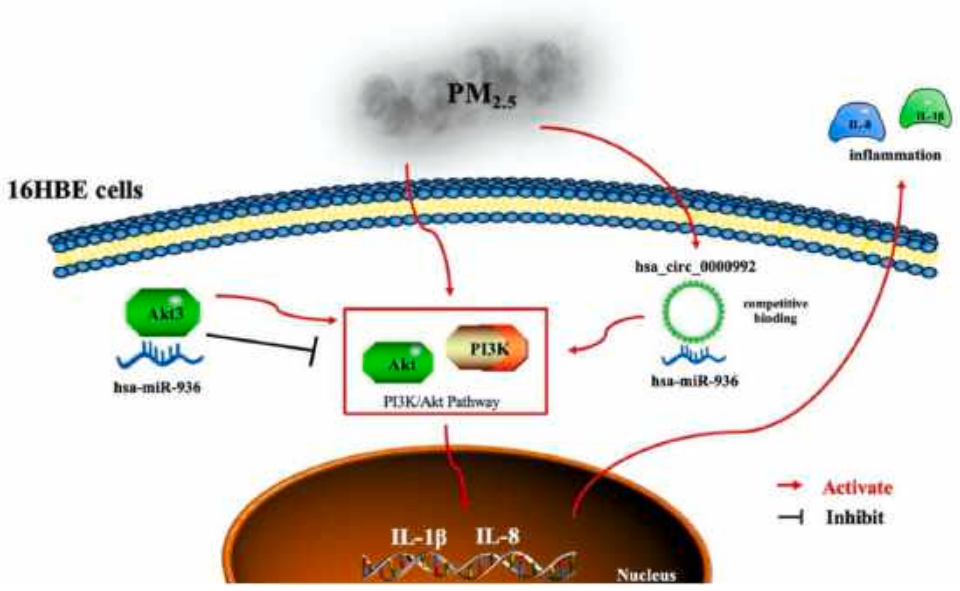

Fig. 15. the mechanism schematic diagram of $PM_{2.5}$-induced inflammation in 16HBE.

Acknowledgements

This work was supported by the Central Public-Interest Scientific Institution Basal Research Fund (Grant No.PM-zx703–202004-155), the Science and Technology planning project of Guangzhou (Grant No.202002030015), the Central Fund Supporting Nonprofit Scientific Institutes for Basic Research and Development (Grant No. PM-zx703–202204-164), and the National Natural Science Foundation of China (Grant No. 21477045).

Appendix A. Supporting information

Supplementary data associated with this article can be found in the online version at doi:10.1016/j.ecoenv.2023.115778.

References

Atkinson, R.W., Kang, S., Anderson, H.R., et al., 2014. Epidemiological time series studies of $PM_{2.5}$ and daily mortality and hospital admissions: a systematic review and meta-analysis. Thorax 69 (7), 660–665.

Bachmayr-Heyda, A., Reiner, A.T., Auer, K., et al., 2015. Correlation of circular RNA abundance with proliferation—exemplified with colorectal and ovarian cancer, idiopathic lung fibrosis, and normal human tissues. Sci. Rep. 5, 8057.

Bekki, K., Ito, T., Yoshida, Y., et al., 2016. $PM_{2.5}$ collected in China causes inflammatory and oxidative stress responses in macrophages through the multiple pathways. Environ. Toxicol. Pharmacol. 45, 362–369.

Burd, C.E., Jeck, W.R., Liu, Y., et al., 2010. Expression of linear and novel circular forms of an INK4/ARF-associated non-coding RNA correlates with atherosclerosis risk. PLoS Genet 6 (12), e1001233.

Dinarello, C.A., 2018. Overview of the IL-1 family in innate inflammation and acquired immunity. Immunol. Rev. 281 (1), 8–27.

Ding, L., Zhang, L., Kim, M., et al., 2017. Akt3 kinase suppresses pinocytosis of low-density lipoprotein by macrophages via a novel WNK/SGK1/Cdc42 protein pathway. J. Biol. Chem. 292 (22), 9283–9293.

GBD (Global Burden of Disease Study) collaborators, 2015. Global, regional, and national age-sex specific all-cause and cause-specific mortality for 240 causes of death, 1990-2013: a systematic analysis for the Global Burden of Disease Study 2013. Lancet 385 (9963), 117–171.

Ghosal, S., Das, S., Sen, R., et al., 2013. Circ2Traits: a comprehensive database for circular RNA potentially associated with disease and traits. Front. Genet. 4, 283.

Gu, S., Dai, H., Zhao, X., et al., 2020. AKT3 deficiency in M2 macrophages impairs cutaneous wound healing by disrupting tissue remodeling. Aging (Albany NY) 12 (8), 6928–6946.

Guo, C., Zhang, Z., Lau, A.K.H., et al., 2018. Effect of long-term exposure to fine particulate matter on lung function decline and risk of chronic obstructive pulmonary disease in Taiwan: a longitudinal, cohort study. Lancet Planet Health 2, e114–e125.

Guo, J.U., Agarwal, V., Guo, H., et al., 2014. Expanded identification and characterization of mammalian circular RNAs. Genome Biol. 15 (7), 409.

Han, X., Zhuang, Y., 2021. $PM_{2.5}$ induces autophagy-mediated cell apoptosis via PI3K/AKT/mTOR signaling pathway in mice bronchial epithelium cells. Exp. Ther. Med. 21 (1), 1.

Jia, Y., Li, X., Nan, A., et al., 2020. Circular RNA 406961 interacts with ILF2 to regulate $PM_{2.5}$-induced inflammatory responses in human bronchial epithelial cells via activation of STAT3/JNK pathways. Environ. Int. 141, 105755.

Jo, Y.S., Lim, M.N., Han, Y.J., et al., 2018. Epidemiological study of $PM_{2.5}$ and risk of COPD-related hospital visits in association with particle constituents in Chuncheon, Korea. Int. J. Chron. Obstruct. Pulmon. Dis. 13, 299–307.

Khan, J.Z., Sun, L., Tian, Y., et al., 2021. Chemical characterization and source apportionment of PM_1 and $PM_{2.5}$ in Tianjin, China: impacts of biomass burning and primary biogenic sources. J. Environ. Sci. (China) 99, 196–209.

Li, M., Hua, Q., Shao, Y., et al., 2020. Circular RNA circBbs9 promotes $PM_{2.5}$-induced lung inflammation in mice via NLRP3 inflammasome activation. Environ. Int. 143, 105976.

Li, P., Xin, J., Wang, Y., et al., 2013. The acute effects of fine particles on respiratory mortality and morbidity in Beijing, 2004–2009. Environ. Sci. Pollut. Res. Int 20 (9), 6433–6444.

Li, R., Wang, Y., Song, X., et al., 2018. Potential regulatory role of circular RNA in idiopathic pulmonary fibrosis. Int. J. Mol. Med. 42 (6), 3256–3268.

Li, X., Li, J., Zhang, Y., et al., 2021. The role of IL-8 in the chronic airway inflammation and its research progress. J. Clin. Otorhinolaryngol. Head. Neck Surg. 35 (12), 1144–1148.

Lin, X.J., Liu, H., Li, P., et al., 2020. miR-936 suppresses cell proliferation, invasion, and drug resistance of laryngeal squamous cell carcinoma and targets GPR78. Front. Oncol. 10, 60.

Liu, Q., Zhang, X., Hu, X., et al., 2017. Emerging roles of circRNA related to the mechanical stress in human cartilage degradation of osteoarthritis. Mol. Ther. Nucleic Acids 7, 223–230.

Longhin, E., Holme, J.A., Gualtieri, M., et al., 2018. Milan winter fine particulate matter ($wPM_{2.5}$) induces IL-6 and IL-8 synthesis in human bronchial BEAS-2B cells, but specifically impairs IL-8 release. Toxicol. Vitr. 52, 365–373.

Memczak, S., Jens, M., Elefsinioti, A., et al., 2013. Circular RNAs are a large class of animal RNAs with regulatory potency. Nature 495 (7441), 333–338.

Mukherjee, A., Agrawal, M.A., 2018. Global perspective of fine particulate matter pollution and its health effects. Rev. Environ. Contam. Toxicol. 244, 5–51.

Nan, A., Chen, L., Zhang, N., et al., 2017. A novel regulatory network among LncRpa, CircRar1, MiR-671 and apoptotic genes promotes lead-induced neuronal cell apoptosis. Arch. Toxicol. 91 (4), 1671–1684.

Qiao, L., Cai, J., Wang, H., et al., 2014. $PM_{2.5}$ constituents and hospital emergency-room visits in Shanghai, China. Environ. Sci. Technol. 48 (17), 10406–10414.

Qin, S., Li, B., Wang, X., et al., 2020. Metal element detection and carcinogenicity risk assessment of PM(2.5) samples. Environ. Toxicol. Chem. 39 (6), 1273–1276.

Revathidevi, S., Munirajan, A.K., 2019. Akt in cancer: mediator and more. Semin. Cancer Biol. 59, 80–91.

Salzman, J., Chen, R.E., Olsen, M.N., et al., 2013. Cell-type specific features of circular RNA expression. PLoS Genet. 9 (9), e1003777.

Shang, Y., Sun, Z., Cao, J., et al., 2013. Systematic review of Chinese studies of short-term exposure to air pollution and daily mortality. Environ. Int. 54, 100–111.

Tan, Y., Wang, Y., Zou, Y., et al., 2020. LncRNA LOC101927514 regulates $PM_{2.5}$-driven inflammation in human bronchial epithelial cells through binding p-STAT3 protein. Toxicol. Lett. 319, 119–128.

Traboulsi, H., Guerrina, N., Iu, M., et al., 2017. Inhaled pollutants: the molecular scene behind respiratory and systemic diseases associated with ultrafine particulate matter. Int. J. Mol. Sci. 18 (2), 243.

Wang, D.H., Zhou, P.Y., Jiang, C.X., et al., 2021. Effects of atmospheric fine particulate matter on respiratory system. Sci. Technol. Vis. 2021 (06), 103–104.

Xian, M., Wang, K., Lou, H., et al., 2019. Short-term haze exposure predisposes healthy volunteers to nasal inflammation. Allergy Asthma Immunol. Res. 11, 632–643.

Xing, Y.F., Xu, Y.H., Shi, M.H., et al., 2016. The impact of $PM_{2.5}$ on the human respiratory system. J. Thorac. Dis. 8 (1), E69–E74.

Xu, J., Srivastava, D., Wu, X., et al., 2021. An evaluation of source apportionment of fine OC and $PM_{2.5}$ by multiple methods: APHH-Beijing campaigns as a case study. Faraday Discuss. 226, 290–313.

Yang, J., Cheng, M., Gu, B., et al., 2020. CircRNA_09505 aggravates inflammation and joint damage in collagen-induced arthritis mice via miR-6089/AKT1/NF-κB axis. Cell Death Dis. 11 (10), 833.

Yang, X., Wang, J., Zhou, Z., et al., 2018. Silica-induced initiation of circular ZC3H4 RNA/ZC3H4 pathway promotes the pulmonary macrophage activation. FASEB J. 32 (6), 3264–3277.

Yang, Y., Li, Z., Yuan, H., et al., 2019. Reciprocal regulatory mechanism between miR-214-3p and FGFR1 in FGFR1-amplified lung cancer. Oncogenesis 8 (9), 50.

Yao, Y., Wang, H., Xi, X., et al., 2021. miR-150 and SRPK1 regulate AKT3 expression to participate in LPS-induced inflammatory response. Innate Immun. 27 (4), 343–350.

Yeung, Y.T., Aziz, F., Guerrero-Castilla, A., et al., 2018. Signaling pathways in inflammation and anti-inflammatory therapies. Curr. Pharm. Des. 24 (14), 1449–1484.

Zhang, F., Ma, H., Wang, Z.L., et al., 2020. The PI3K/AKT/mTOR pathway regulates autophagy to induce apoptosis of alveolar epithelial cells in chronic obstructive pulmonary disease caused by $PM_{2.5}$ particulate matter. J. Int. Med. Res. 48 (7), 300060520927919.

Zhang, H.D., Jiang, L.H., Sun, D.W., et al., 2018. CircRNA: a novel type of biomarker for cancer. Breast Cancer 25 (1), 1–7.

Zhang, Q., Quan, J., Tie, X., et al., 2015. Effects of meteorology and secondary particle formation on visibility during heavy haze events in Beijing. China Sci. Total Environ. 502, 578–584.

Zhao, S., Tian, H., Luo, L., et al., 2021. Temporal variation characteristics and source apportionment of metal elements in PM(2.5) in urban Beijing during 2018–2019. Environ. Pollut. 268 (Pt B), 115856.

Zhou, C., Tan, Y., Wang, Y., et al., 2020. $PM_{2.5}$-inducible long non-coding RNA (NONHSAT247851.1) is a positive regulator of inflammation through its interaction with raf-1 in HUVECs. Ecotoxicol. Environ. Saf. 196, 110476.

Zhou, X., Tao, H., 2018. Overexpression of microRNA-936 suppresses non-small cell lung cancer cell proliferation and invasion via targeting E2F2. Exp. Ther. Med. 16 (3), 2696–2702.

Zhu, X., Zhao, P., Lu, Y., et al., 2019. Potential injurious effects of the fine particulate $PM_{2.5}$ on the progression of atherosclerosis in apoE-deficient mice by activating platelets and leukocytes. Arch. Med. Sci. 15 (1), 250–261.